MATRIX SIGN ALGORITHM FOR SINUSOIDAL FREQUENCY AND DOA ESTIMATION PROBLEMS

Mohammed A. Hasan† and Jawad A. Hasan*
†Dept. of Electrical & Computer Engineering, University of Minnesota, Duluth, MN 55812
*Dept. of Electrical Engineering, University of Baghdad, Baghdad, Iraq
E.mail: mhasan@d.umn.edu

ABSTRACT

Fast algorithms based on the matrix sign function are developed to estimate the signal and noise subspaces of the sample correlation matrices. These subspaces are then utilized to develop high resolution methods such as MUSIC and ESPRIT for sinusoidal frequency and direction of arrival (DOA) problems. The main feature of these algorithms is that they generate subspaces that are parameterized by the signal-to-noise ratio (SNR). Significant computational saving will be obtained due to the fast convergence of these higher order iterations and to the fact that subspaces rather than individual eigenvectors are actually computed. Simulations showing the performance of these methods were also presented.

1. INTRODUCTION

In most applications of subspace methods in sinusoidal and direction of arrival estimation problems, the signal or noise subspace is required rather than the individual eigenvectors to derive high resolution methods such as MUSIC and ESPRIT. These subspaces are traditionally computed using eigendecomposition or (singular value decomposition) of the covariance matrix of the data. Both of these techniques require explicit computations of eigen (singular) vectors and eigen (singular) values. A considerable computational effort can be achieved if these subspaces are computed without the need to compute the associated eigenvalues or eigenvectors. In this paper we propose efficient subspace separation methods which can be implemented using matrix sign function algorithms. The most salient features of these algorithms are that they are globally convergent in that they converge from almost any initial condition (in the sense of probability one). Second, a technique is available which generates rth order algorithms for any $r \geq 2$. They are also self correcting in that any mistake in one step of the computations will be corrected in the subsequent steps. All these features combined together provide a close to ideal algorithms for subspace computation. In this paper we show that the matrix sign function provides a good tool for deriving such algorithms.

The matrix sign function is a special case of the matrix sector function and is thoroughly studied in the literature. The matrix sign function has a wide range of applications in approximation and computational methods, control theory, eigendecomposition and spectral theory. It is also used in the computations of roots of matrices and sector functions [1]-[2] and [4]-[5]. In [12] the matrix sign function was utilized for the separation of eigenvalues in specific regions in the complex plane such as squares and rectangles. A comprehensive presentation of the history of the matrix sign function including its applications and computation in the last two decades is given in [7]-[10].

Let $A \in \mathcal{C}^{m\times m}$ be diagonalizable nonsingular matrix having no negative eigenvalue such that $P^{-1}AP = \mathrm{diag}(\lambda_1, \cdots, \lambda_m)$, then the matrix sign function is defined as $S = \mathrm{sign}(A) = P^{-1}\mathrm{diag}(\mathrm{sign}(\lambda_1), \cdots, \mathrm{sign}(\lambda_m))P$, where for any $z = x + iy \in \mathcal{C}$ with $x \neq 0$,

$$\mathrm{sign}(z) = \mathrm{sign}(x+iy) = \mathrm{sgn}(x) \qquad (1a)$$

$$\mathrm{sgn}(x) = \begin{cases} 1 & \text{if } x > 0, \\ -1 & \text{if } x < 0. \end{cases} \qquad (1b)$$

Note that $S^2 = I$ and $SA = AS$. Thus the sign function algorithm will map eigenvalues with positive real parts to 1 and those with negative real parts to -1. Note that sign(A) is not defined when A is singular.

2. MATRIX SIGN FUNCTION METHOD

In this section we develop fast and efficient algorithms for computing the matrix sign function of complex matrices. To derive higher order fixed point iteration for computing the matrix sign functions let $C_r(Y)$ and $D_r(Y)$ be polynomial matrices defined as

$$C_r(Y) = \sum_{l=0}^{[\frac{r}{2}]} \binom{r}{2l} Y^{r-2l} \qquad (2a)$$

$$D_r(Y) = \sum_{l=0}^{[\frac{r}{2}]} \binom{r}{2l+1} Y^{r-2l-1}, \qquad (2b)$$

where $[\frac{r}{2}]$ is the largest integer less than or equal to $\frac{r}{2}$.

For each positive integer r we define $\Phi_r(Y) = D_r(Y)^{-1}C_r(Y)$. When $r = 2$, this reduces to the standard Newton method where $C_2(Y) = Y^2 + I$ and $D_2(Y) = 2Y$ and hence $\Phi_2(Y) = (2Y)^{-1}(Y^2 + I)$. In the next result some properties of Φ_r are presented.

Theorem 1. *Let A and S be nonsingular matrices and let S be the matrix sign function of A. Let C_r and D_r be as defined in (2) for $r \geq 2$. Let $\Phi_1(Y) = Y$, then for $r > 1$, Φ_r can recursively be generated as follows*

$$\Phi_r(Y) = \{\Phi_{r-1}(Y) + Y\}^{-1}\{Y\Phi_{r-1}(Y) + I_m\}, \quad (3a)$$

and for $1 \leq l < r$,

$$\Phi_r(Y) = \{\Phi_{r-l}(Y) + \Phi_l(Y)\}^{-1}\{\Phi_l(Y)\Phi_{r-l}(Y) + I_m\}. \qquad (3b)$$

Moreover, Φ_r satisfy the following

(i) $\Phi_r(Y) = \{(Y+S)^r - (Y-S)^r\}^{-1}\{(Y+S)^r + (Y-S)^r\}S$.

(ii) $\Phi_r(Y) = S + (2S)^{-r+1}(Y-S)^r + O(Y-S)^{r+1}$.

(iii) $\Phi_{2r}(Y) = (2\Phi_r(Y))^{-1}(\Phi_r^2(Y) + I_m)$.

(iv) $\Phi_{nr}(Y) = \{D_n(\Phi_r(Y)\}^{-1}\{C_n(\Phi_r(Y))\}$.

(v) $\Phi_r(\Phi_s(Y)) = \Phi_s(\Phi_r(Y)) = \Phi_{rs}(Y)$.

(vi) $\Phi_{r^2}(Y) = \Phi_r(\Phi_r(Y))$.

(vii) $\Phi_{r^l}(Y) = \Phi_r(\Phi_r(\cdots(\Phi_r(Y)))$.

(viii) *Φ_r satisfy the following initial value problem* $\frac{d}{dY}\Phi_r(Y) = r\{(Y-S)(Y+S)\}^{-1}\{(\Phi_r(Y) - S)(\Phi_r(Y) + S)\}$ with $\Phi_r(S) = S$.

Additionally, $\Phi_r(Y)$ is odd for all positive integers $r \geq 1$.

Proof. See [3].

The notation $O(x)$ means that $\frac{O(x)}{x}$ remains bounded near $x = 0$. Using this theorem we will generate a fixed point function of order $r \geq 2$ which will be used later to compute the matrix sign function of a nonsingular matrix which is the utilized to compute the signal and noise subspaces. Based on the last theorem, one may develop the following algorithm.

Algorithm 1

(i) Set $Y_0 = A$ and choose $r \geq 2$

For $k = 1 : N$

(ii) $C_r(Y_k) = \sum_{l=0}^{[\frac{r}{2}]} \binom{r}{2l} Y_k^{r-2l}$

(iii) $D_r(Y_k) = \sum_{l=0}^{[\frac{r}{2}]} \binom{r}{2l+1} Y_k^{r-2l-1}$

(iv) $Y_{k+1} = D_r(Y_k)^{-1}C_r(Y_k)$

It can be shown from Theorem 1 that the error formula for the above algorithm has the form

$$(Y_{k+1} - S)(Y_{k+1} + S)^{-1} = \{(Y_k - S)(Y_k + S)^{-1}\}^r.$$

As can easily be seen from this error formula, the convergence of Algorithm 1 is rth order. Also it was obseved from several simulations that for most practical applications $N = 3$ or 4 is sufficient to achieve convergence to the matrix sign function.

3. APPLICATIONS TO SINUSOIDAL AND DOA PROBLEMS

The sinusoidal frequency and DOA estimation problems are of interest in many applications in radar, sonar, and seismology. Several approaches have been developed over the years and among the well-known approaches to this problem are the matrix pencils and subspace methods [6] and [12]-[14]. The DOA problem can be formulated as follows. Consider a linear array of p sensors and q multiple narrow-band signals impinging on the array with DOA angles $\theta_1, \theta_2, \cdots, \theta_q$. Assuming that p snapshots are available, the received signal at the array can be expressed as

$$\mathbf{x}(k) = A(\theta)\mathbf{s}(k) + \mathbf{v}(k), \qquad (4a)$$

where $\mathbf{s}(k) \in \mathcal{C}^q$ ($\mathcal{C}$ is the field of complex numbers) is a vector of complex signals of q wavefronts

$$\mathbf{s}(k) = [\, s_1(k) \quad s_2(k) \quad \cdots \quad s_q(k) \,]^T, \qquad (4b)$$

$\mathbf{v}(k)$ is a $p \times 1$ vector of additive noise in sensors with

$$\mathbf{v}(k) = [\, v_1(k) \quad v_2(k) \quad \cdots \quad v_p(k) \,]^T, \qquad (4c)$$

and A is $p \times q$ matrix

$$A(\theta) = [\, \mathbf{a}(\theta_1) \quad \mathbf{a}(\theta_2) \quad \cdots \quad \mathbf{a}(\theta_q) \,], \qquad (4d)$$

with $\mathbf{a}(\theta) = [1 \quad e^{jw(\theta)} \quad e^{j2w(\theta)} \quad \cdots \quad e^{j(p-1)w(\theta)}]^T$ being the steering vector of the array toward the direction θ. Here $w(\theta)$ is some known function which is solvable for θ. It is also assumed that the signals and additive noise are zero-mean stationary complex-valued random processes such that $E[v_i(k)v_j^*(k)] = \sigma_v^2\delta_{i-j}$ for $i = 1, \cdots, q$, where σ_v^2 is the variance of v. Here $E[.]$ and * denote the expectation, and conjugate transpose operators, respectively. Thus, the spatial $p \times p$ covariance matrix of the array output is given by $R_x := E[\mathbf{x}(k)\mathbf{x}^*(k)] = A(\theta)R_sA(\theta)^* + \sigma_v^2 I_p$ with $R_s = E[\mathbf{s}(k)\mathbf{s}^*(k)]$ is $q \times q$ covariance matrix of s and I_p is the $p \times p$ identity matrix. Note that the minimum eigenvalue of R_x is equal to σ_v^2 with multiplicity $p - q$.

The frequency estimation problem can be posed as the determination of a set of complex sinusoids from the measured output $x(k)$ in the presence of measurement noise, i.e.,

$$x(k) = s(k) + v(k), \tag{5a}$$

where

$$s(k) = \sum_{i=1}^{q} A_i e^{-j2\pi k f_i}, \tag{5b}$$

and the noise process $v(k)$ is assumed to be independent of $x(k)$, A_i, and f_i are the amplitude, and frequency of the ith complex sinusoid, respectively.

The methods discussed in this paper will handle both types of problems, the DOA in (4) and sinusoidal frequency estimation (5).

Let $\hat{R}_x$ be the sample covariance matrix of $x(k)$ and assume that the eigenvalues of $\hat{R}_x$ are sorted in decreasing order so that $\lambda_1 \geq \lambda_2 \cdots \geq \lambda_q > \lambda_{q+1} = \cdots = \lambda_p = \sigma_v^2$ with corresponding eigenvectors $\{\mathbf{u}_i\}_{i=1}^p$. The eigenvectors $\{\mathbf{u}_i\}_{i=1}^q$ are usually called the signal vectors which span the signal subspace with projection $U_sU_s^* = \sum_{i=1}^q \mathbf{u}_i\mathbf{u}_i^*$ and the eigenvectors $\{\mathbf{u}_i\}_{i=q+1}^p$ are called the noise vectors which span the noise subspace with projection $U_nU_n^* = \sum_{i=q+1}^p \mathbf{u}_i\mathbf{u}_i^*$. When the noise $v(k)$ is white process, $A(\theta)R_sA^*(\theta) = U_s\Lambda^2U_s^*$, where $\Lambda = \text{diag}(\lambda_1, \lambda_2, \cdots, \lambda_q)$ and hence $A(\theta)R_s^{\frac{1}{2}} = U_s\Lambda V$ for some orthogonal matrix V. Therefore, $U_n^*A(\theta)R_s^{\frac{1}{2}} = U_n^*U_s\Lambda V = 0$ from which it follows $U_n^*A(\theta_i) = 0$ or equivalently $\{\mathbf{u}_i\}_{i=q+1}^p$ are orthogonal to $\{\mathbf{a}(\theta_i)\}_{i=1}^q$. The signal subspace is spanned by $\{\mathbf{a}(\theta_i)\}_{i=1}^q$ and thus the last relation simply means that the vectors $\{\mathbf{u}_i\}_{i=q+1}^p$ span the noise subspace.

Since $\hat{R}_x$ is positive definite, all its eigenvalues are non-negative and thus the matrix sign function of $\hat{R}_x$ is I_p. In this case we have to use a shifted version of the sign function algorithm. Let $\tilde{R}_x = \hat{R}_x - \eta tr(\hat{R}_x)I_p$. The number η is empirical and is dependent on applications and signal-to-noise ratio (SNR). In our simulations we used $0 \leq \eta \leq 0.2$. This implies that the pure signal energy is 80% of the total energy. Thus the matrix sign algorithm maps the matrix $\hat{R}_x$ into $U = U_s - U_n$ with $U_s + U_n = I$. Therefore $U_s = \frac{I+U}{2}$ and $U_n = \frac{I-U}{2}$. Here U_s are orthogonal matrices whose columns are the eigenvectors corresponding to the positive and negative eigenvalues of $\tilde{R}_x$, respectively. Once the signal and noise subspaces are estimated, high resolution methods such as MUSIC, ESPRIT, or Root-MUSIC can be used to determine the frequencies.

4. SIMULATIONS

Several data sets were generated using the equation

$$x(k) = A_1e^{-j2\pi f_1 k} + A_2e^{-j2\pi f_2 k} + v(k), \tag{6}$$

where $A_1 = 1.0$, $A_2 = 1.0$, $f_1 = 0.5$, $f_2 = 0.52$ and $k = 1, 2, \cdots, 25$. Note that $f_2 - f_1 = .02$ which is less than $\frac{1}{25} = 0.04$, the Fourier frequency. The SNR for either sinusoids is defined as $10\log_{10}(\frac{\sigma_s^2}{\sigma_v^2})$, where $s(k) = A_1e^{-j2\pi f_1 k} + A_2e^{-j2\pi f_2 n}$ and σ_s^2, σ_v^2 are the variances of $s(k)$ and $v(k)$, respectively. The additive noise was colored and generated by passing a complex white Gaussian process of unit variance through an FIR filter with impulse response $\{1, 1, 1\}$. The size of each matrix was chosen to be p=15 which in the presence of Gaussian noise has effective rank two. The matrix sign function algorithm based on Theorem 1 with $r = 2$ was used for the computation of the signal subspace and noise subspaces. Figures 1 and 2 display the peaks for SNR=5, 0 dB using the covariance matrix of size $p = 15$ and $\eta = 0.2$. One can see from these figures that a fairly accurate results can be obtained even for very close sinusoids at low SNR and the presence of colored noise.

5. CONCLUSION

The purpose of this article has been to develop several robust and numerically efficient methods for the computation of the principal subspaces required in deriving high resolution methods for sinusoidal frequency and direction of arrival estimation problems. These principal subspaces were derived using higher order iterations for computing the matrix sign function of complex matrices. Specifically, given any positive integer $r \geq 2$, we presented a systematic way of deriving rth order convergent algorithms. For $r = 2$, and $r = 3$, the techniques of this paper become the Newton' and Halley's methods respectively for solving the equations $S^2 = I$ and $SA = AS$.

References

[1] Blazer L. A., "Accelerated Convergence of the Matrix Sign Function Method of Solving Lyapunov, Riccati and Other Equations," *Int. J. Control*, Vol. 32, No. 6, pp. 1076-1078, 1980.

[2] Denman E. D. and Beavers A. N., "The Matrix Sign Function and Computation of Systems," *Appl. Math. Comput.*, Vol. 2, pp. 63-94, 1976.

[3] Hasan M. A., "Higher Order Matrix Sign Function Algorithms for Solving the Algebraic Riccati and Lyapunov Equations," submitted.

[4] Hoskins W. D. and Walton D. J., "A Faster, More Stable Method for Computing the pth Root of Positive Definite Matrices," *Linear Algebra Appl.*, Vol. 26, pp. 139-163,1979.

[5] Hoskins W. D. and Walton D. J., "A Faster Method of Computing the Square Root of a Matrix," *IEEE Trans. Automatic. Contr.*, Vol. AC-23, No. 3, pp. 494-495, 1978.

[6] Y. Hua Y. and Sarkar T. K., "On SVD for Estimating Generalized Eigenvalues of Singular Matrix Pencils in Noise," *IEEE Trans. on Signal Processing,* Vol. 39, No. 4, pp. 892-899, April 1991.

[7] Kenney C., and Laub A. J., "Rational Iterative Methods for the Matrix Sign Function", *SIAM J. Matrix Anal. Appl.*, Vol 12., pp. 237-291, April 1991.

[8] Kenney C. S., Laub A. J., and Papadopoulos P. M., A Newton-Squaring Algorithm for Computing the Negative Invariant Subspace of a Matrix, *IEEE Trans. Automatic Control*, Vol. 38, No. 8, pp. 1284-1289, August 1993.

[9] Kenney C. S. and Laub A. J., The Matrix Sign Function, *IEEE Trans. Automatic Control*, Vol. 40, No. 8, pp. 1330-1348, August 1995.

[10] Koc C. K., Bakkaloglu B., and Shieh L. S., "Computation of the Matrix Sign Function Using Continued Fraction Expansion," *IEEE Trans. Automatic Control*, Vol. AC-39, No. 8, pp. 1644-1647, Aug.1994.

[11] Stickel E. U., Separating Eigenvalues Using the Matrix Sign Function, *Linear Algebra Appl.*, 148, pp. 75-88, 1991.

[12] Stoica P., and Soderstrom T. and Ti F., "Asymptotic Properties of the High-Order Yule-Walker Estimates of Sinusoidal Frequencies," *IEEE Trans. Signal Processing,* Vol. 37, No. 11, pp. 1721-1734, November 1989.

[13] Stoica P., and Soderstrom T., "Statistical Analysis of MUSIC and Subspace Rotation Estimates of Sinusoidal Frequencies'" *IEEE Trans. Signal Processing,* Vol. 39, No. 8, pp. 1836-1847, August 1991.

[14] D. W. Tufts and R. Kumaresan, "Estimation of Frequencies of Multiple Sinusoids; Making Linear Prediction Perform Like Maximum Likelihood," Proc. IEEE, Vol. 70, pp. 975-989, Sept. 1982.

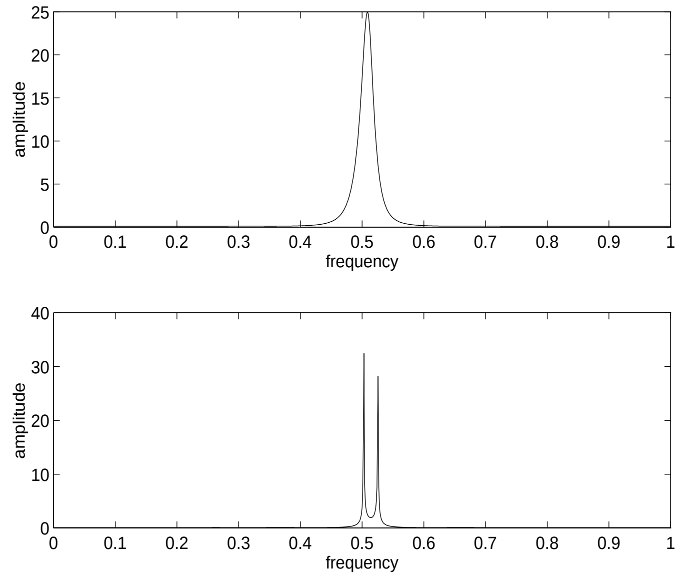

Figure 1: Spectral peaks at $f_1 = 0.5$ and $f_2 = 0.52$ with $SNR = 5dB$. The top plot resulted from applying exact MUSIC-based estimator, while the bottom was generated using Algorithm 1.

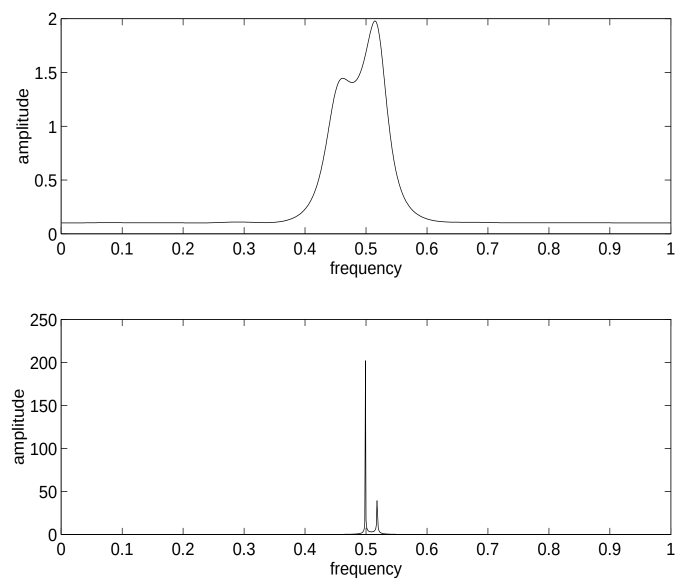

Figure 2: Spectral peaks at $f_1 = 0.5$ and $f_2 = 0.52$ with $SNR = 0dB$. The top plot resulted from applying exact MUSIC-based estimator, while the bottom was generated using Algorithm 1.